SLOVAK UNIVERSITY OF TECHNOLOGY IN BRATISLAVA
Faculty of Electrical Engineering and Information Technology

Ing. Rastislav Ries

Reg. No.: FEI-104400-46711

Superconducting properties and microstructure of thin films for superconducting radiofrequency cavities

Dissertation Thesis Abstract

Study programme: Physical Engineering

Study field: Electrical and Electronics Engineering

Training workplace: Institute of Electrical Engineering SAS

Form of study: Full-time

Bratislava 2021

Dissertation Thesis has been prepared at Institute of Electrical Engineering Slovak Academy of Sciences, Department of Superconductors

Submitter: Ing. Rastislav Ries
Institute of Electrical Engineering SAS
Dúbravská cesta 9,
841 04 Bratislava

Supervisor: doc. Ing. Fedor Gömöry, DrSc.
Institute of Electrical Engineering SAS
Dúbravská cesta 9,
841 04 Bratislava

Consultant: Mgr. Eugen Seiler, PhD
Institute of Electrical Engineering SAS
Dúbravská cesta 9,
841 04 Bratislava

Reviewers: doc. RNDr. Michal Maheľ, CSc.
Comenius University
Mlynská dolina
842 48 Bratislava

Prof. Laura Gozzelino
Politecnico di Torino
Corso Duca degli Abruzzi, 24
10129 Torino
Italy

Dissertation thesis abstract was sent: 15.5.2021
Dissertation Thesis defence will be held on:

Dean of the faculty FEI, STU: prof. Dr. Ing. Miloš Oravec

CONTENTS

Overview

Superconducting radiofrequency (SRF) cavities are electromagnetic resonators which are used to manipulate and accelerate charged particles in particle accelerators. The SRF cavities have specific geometries with resonant frequency designed to match with the electromagnetic waves. The inner surface of the SRF cavity is made by superconducting material providing reflection of the electromagnetic waves which are resonantly excited inside the cavity leading to acceleration of the particle. The SRF cavities are designed to reach the highest possible electric field on the cavity axis with the lowest power dissipation. The maximum electric field is limited by the ability of the superconductor to persist in the Meissner state. The superconductor loses Meissner state if the applied magnetic field reaches the value of the first critical field H_c.

For SRF application, thin Nb film on Cu substrate is one of the alternatives to bulk Nb which is currently the most common material in SRF cavities. The advantage of the Nb/Cu structure is not to exceed bulk Nb in performance, but that Nb/Cu may offer simplifications in cryo-cooling given the better thermal conductivity of Cu compared to Nb, improved mechanical stability and reduced sensitivity to magnetic flux trapping. All these practical implications could offer more economical operation, but research and development is required to achieve reproducible performance that competes with the bulk Nb.

This thesis focused on investigation of different types of Nb/Cu samples for SRF cavities and use of laser irradiation as a tool to improve the SC properties of the Nb thin films. The laser post-treatment of the Nb/Cu samples was first performed by E. Radicioni in 1995 [1]. The laser parameters suitable for irradiation of Nb in all surface conditions expected for cavity production were investigated recently by L. Zhao in 2015 [2]. The progress in laser post-treatment of the Nb for SRF cavities had started only few years ago. The surface topography of the Nb films after laser irradiation was inspected by Y. Yang in 2020 [3], followed that laser irradiation can modify the magnetic hysteresis loops of the Nb observed by A. Cubero in 2020 [4]. The improved adhesion between Nb and Cu after laser post-treatment was investigated by Medvids in 2020 [5]. The effects of laser post-treatment on superconducting and microstructural properties of the Nb/Cu samples are investigated in this thesis considering previous results of other groups.

In this thesis, DC superconducting properties were studied at a temperature 4.2 K for 14 different types of Nb thin films deposited by magnetron sputtering on Cu substrates. The results of superconducting properties of the Nb/Cu samples were compared with microstructural properties obtained by AFM, SEM and XRD. The superconducting and microstructural properties were investigated considering:

a) Different Cu substrate polishing techniques and Nb deposition conditions,

b) Application of laser post-treatment on different types of Nb/Cu samples,

c) Application of different laser energy doses on Nb/Cu samples.

1. Introduction to investigation

The investigations presented in this thesis focused on correlation between superconducting and microstructural properties of the Nb thin films deposited on Cu substrates prepared by the partners involved in the ARIES project [6]. The results in this thesis consider:

a) Influence of 5 different Cu substrate polishing and 3 different Nb deposition conditions. The results of superconducting and microstructural properties of the samples were compared between each other.
b) Influence of the laser post-treatment of the Nb surfaces at constant laser dose (D = 70 J/cm^2) with the comparison of superconducting and microstructural properties before and after laser irradiation.
c) Influence of the laser intensity applying 4 different laser energy doses on two series of Nb samples ($D4$ = 140, $D3$ = 175, $D2$ = 233 and $D1$ = 350 J/cm^2). This includes comparison between the microstructural and superconducting properties of the Nb films before and after irradiation with the different laser energy doses.

The superconducting properties were measured using Vibrating sample magnetometer (VSM) of the commercial Physical Property Measurement System (PPMS). The critical temperature (T_c) of the samples was determined from the magnetic moment vs temperature measurements in the presence of weak constant applied DC field (5 mT). The first magnetic flux entry field (H_{en}), full penetration field (H_p), upper critical field (H_{c2}) and magnetisation width ΔM were determined from initial magnetization curves and magnetic hysteresis loops at constant sample temperature 4.2 K. The VSM measurements in investigation (a) were performed in perpendicular while investigations (b) and (c) in parallel field, as for the SRF application are parallel results more relevant.

The first magnetic flux entry field H_{en} (proportional to H_c through the geometrical constant) was detected as the applied field at which the initial magnetization curve starts to deviate from the linear dependence that the curve follows in the first part starting from the zero applied fields [7] [8]. The field H_{en} was determined employing a 2% relative difference criterion, i.e. as the applied field at which the relative difference between the magnetization curve and the linear Meissner trend reaches 2% (Fig. 1).

The full penetration field (H_p) was determined from the initial magnetization curves as the applied field at which the minimum magnetic moment (maximum in absolute value) is reached. The H_p value is one of the indicators of the overall strength of the flux pinning in the sample, a higher difference between H_{en} and H_p indicates a stronger pinning.

The upper critical field H_{c2} was determined as the applied magnetic field at which the initial magnetization curve reaches the constant dependence at almost-zero magnetic moment in the region of high fields.

The magnetization of the samples was analysed to investigate their pinning behaviour and the critical current density. Larger magnetization width ΔM at a certain magnetic field indicates stronger bulk pinning and higher pinning-based critical current density.

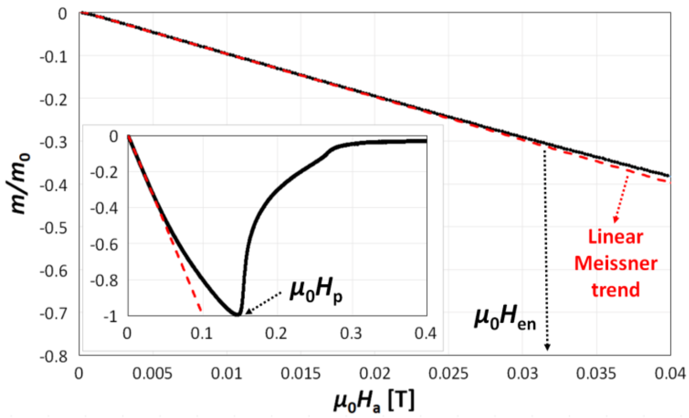

Fig. 1: Initial magnetization curve of the superconducting sample normalized to maximum magnetic moment m_0 illustrating determination of the H_{en} and H_p characteristic fields [9].

2. Effect of Cu substrate polishing and deposition conditions of Nb film

In the Nb film production process a great attention was paid to the preparation of the Cu substrate because its roughness and morphology are expected to be replicated by the growing Nb film. The production of the Nb/Cu samples was divided according to polishing procedures of the Cu substrates and Nb film deposition conditions (Table 1). The Cu polishing procedures were carried out at CERN (chemical polishing SUBU5 as a reference) and INFN (SUBU5 with different recipe as used at CERN, Electropolishing (EP), combination of double polishing procedure EP + SUBU5 and Tumbling) [10]. Thin Nb films were deposited from one side on Cu substrates at 3 different facilities: INFN, UNI Siegen and STFC.

Table 1: Nb/Cu samples preparation table. Vertical direction shows polishing technique applied on Cu substrate. Horizontal direction shows institution at which deposition of the Nb films was performed.

	Cu polishing				
Nb deposition	SUBU5 (CERN)	SUBU5 (INFN)	Electropolishing (INFN)	EP + SUBU5 (INFN)	Tumbling (INFN)
INFN Legnaro	C10	L20	L21	L16	L8
UNI Siegen	C1	L1	L10	L23	L9
STFC Daresbury	C7	L19	L13	L16	

After deposition processes, the Nb/Cu samples were delivered to IEE Bratislava for microstructural and superconducting characterization. As the space in the sample holder of the VSM has some limitations, the initial received samples were cut to approx. 2×2 mm^2.

The critical temperatures of the samples deposited at the certain facility showed almost identical values of T_c. The T_c of the samples deposited at UNI Siegen ranges from 9.6 – 9.7 K, for samples deposited at STFC it is 9.3 – 9.4 K. Samples deposited at INFN showed T_c of about 9.3 K except of sample L20 with the critical temperature 9.6 K. The reason of this deviation is that the L20 sample was sputtered at 580°C instead of 650°C, because during the baking process one of the two infrared lamps was broken. It is obvious that deposition parameters had major effect on T_c of the samples rather than different Cu substrate polishing.

Fig. 2 shows results of H_{en} and H_p for all 14 Nb/Cu samples according to Cu substrate polishing and according to facility of the Nb film deposition.

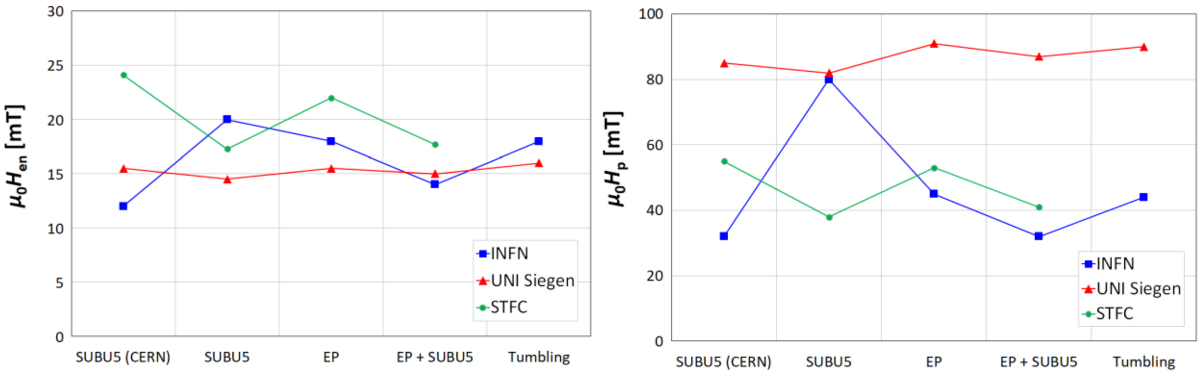

Fig. 2: The results of H_{en} and H_p for all 14 Nb/Cu samples according to Cu substrate polishing and according to facility of the Nb film deposition.

Considering the results of H_{en} and $H_{p,}$ the samples which Cu substrates were polished by SUBU5 (CERN) showed higher values comparing to those of polished by SUBU5 at INFN except of L20 sample. Surprisingly, the L20 sample showed very good results of H_{en} and H_p as expected, despite the fact that deposition temperature was lower (580°C) than it should have been (650°C). Somewhat improved were results of H_{en} and H_p at a samples polished by the EP and Tumbling comparing to results of double polishing techniques EP + SUBU5.

However, there is still dominated factor of Nb deposition conditions mostly visible at UNI Siegen samples. The H_{en} and H_p results of UNI Siegen samples showed almost identical values with very weak changes according to different Cu substrate polishing techniques. The values of H_{en} and H_p of the samples deposited at STFC showed higher values in all cases compared to INFN samples (except of L20 sample). The H_{en} fields of the samples deposited at STFC are higher in all cases compared to UNI Siegen samples.

The $M(H)$ measurements showed that curves for each deposition facility are very similar reflecting the similar pinning strength and critical current density of the Nb films.

It cannot be straightforwardly concluded which polishing technique is optimal considering known data from the investigation, as the highest H_{en} value showed the sample C7 (H_{en} = 24.1 mT) deposited at STFC which Cu was polished by SUBU5 (CERN), but the same polishing technique was used in the sample C10 (H_{en} = 12 mT) deposited at INFN showing the lowest H_{en}. However, the highest average value of the H_{en} showed the samples which Cu was polished by EP. The samples deposited by deposition conditions used at STFC showed in average the best results of H_{en}. Considering results of T_c, H_{en}, H_p, H_{c2} and magnetizations of the samples, it can be concluded that the final superconducting properties of the samples were mostly given by the Nb deposition conditions with a weak effect of Cu substrate polishing.

3. Effect of laser post-treatment applied on Nb surfaces

The INFN samples were chosen for laser post-treated in order to improve their surfaces. The Q-switched pulsed Nd:YAG laser (model: NL301G) was used with constant energy dose D = 70 J/cm^2 applied on the Nb surfaces. Fig. 3 shows values of H_{en}, H_p and H_{c2} after laser post-treatment relative to the results of the non-irradiated samples.

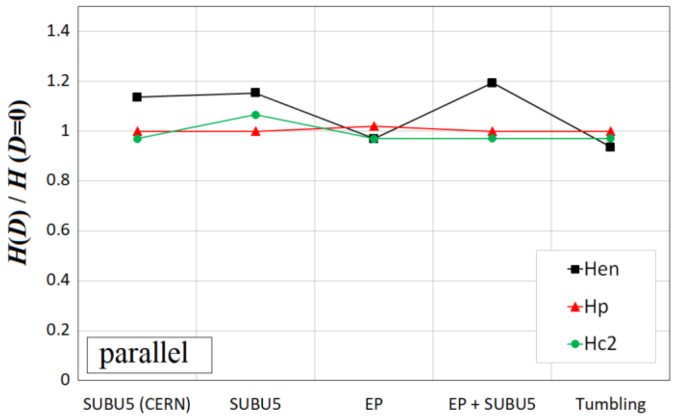

Fig. 3: The relative changes of H_{en}, H_p and H_{c2} after laser-post treatment of the INFN samples.

After laser post-treatment, the H_{en} fields were increased mostly in the samples C10 (+14%), L20 (+16%) and L16 (+19%). The H_{en} fields of the samples L21 and L8 were changed very little after laser post-treatment. In the case of H_p and H_{c2} values, they were changed very little after laser post-treatment in all 5 samples. Compared to non-irradiated sample the magnetization behaviour $M(H)$ showed very little changes after laser post-treatment by D = 70 J/cm^2.

SEM micrographs of the surface morphology of the INFN samples before and after laser irradiation are shown in Fig. 4. As the Cu substrates of the samples were polished by different techniques, they presented some characteristics for each Nb surface. The pits created by application of SUBU5 on Cu and were presented on Nb surfaces C10 (a), L20 (c) and L16 (g). The diameter of pits observed on these surfaces ranges from 0.2 to 3 μm. The surface of the L8 (i) sample contains scratches which were created by the centrifugal polishing (tumbling) with silica and coconut powder.

All the samples irradiated by laser look smoother with visibly molten Nb film. The pitting is no more presented on the Nb surfaces indicating that the pits were completely or partially filled by molten Nb in all 3 cases (C10, L20 and L16). The L21 sample shows well smoothed surface with almost complete removal of the initial surface imperfections after laser irradiation (g). The surface of the L8 sample showed almost complete removal of the scratches after laser irradiation, but cracks emerged on its surface as a consequence of rapid solidification [2] [3]. As shown from the figures, the samples C10, L20 and L16 which exhibited significant increase in H_{en} show also most improved surfaces morphology, reduction of the defects and no additional defect formation after the laser post-treatment.

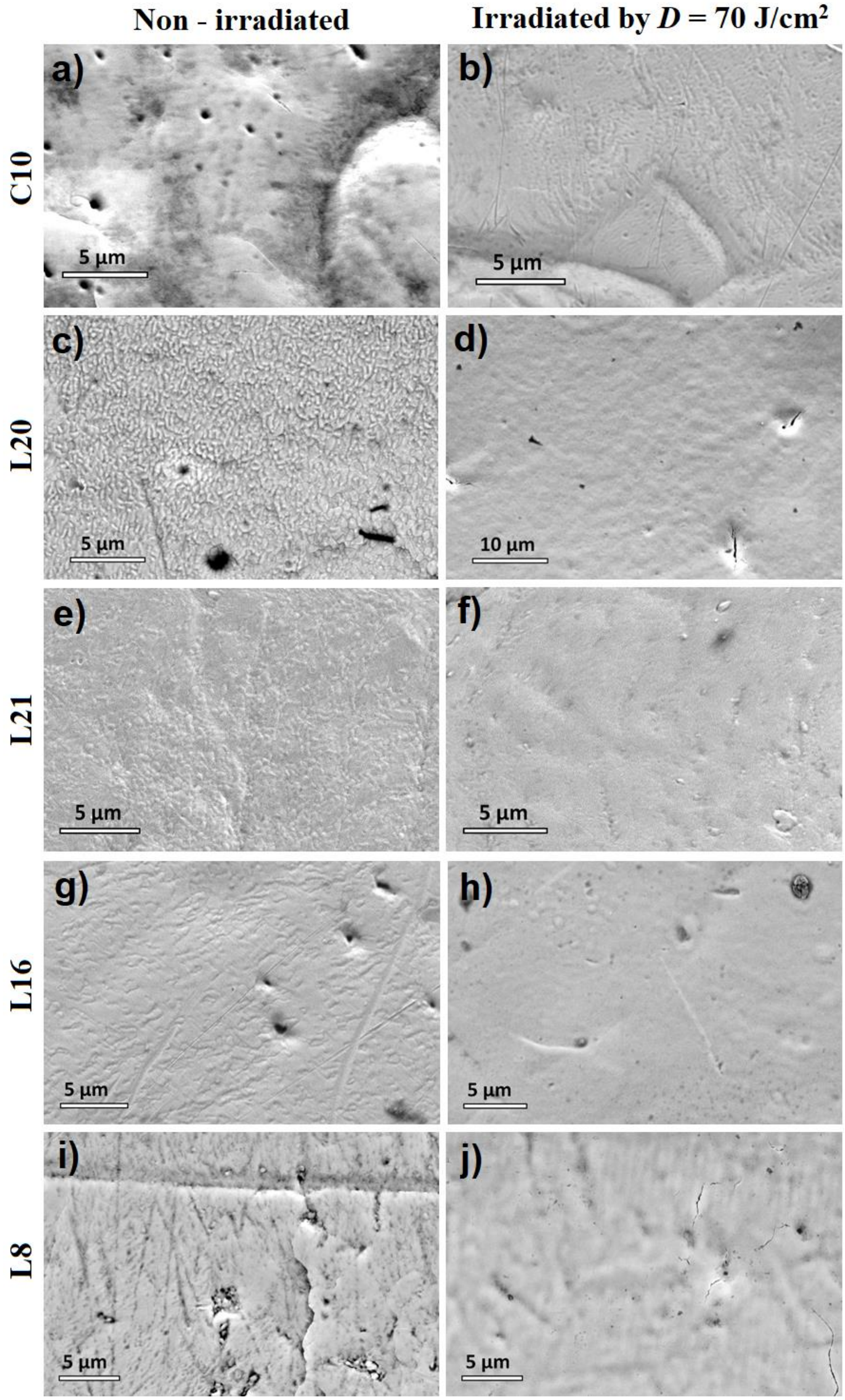

Fig. 30: SEM micrographs of INFN samples before and after laser post-treatment by energy dose D = 70 J/cm^2.

4. Effect of different Laser doses applied on Nb surfaces

The samples L16 and L20 were chosen for irradiation by laser at 4 different laser doses to investigate effect of different energy doses applied on Nb surfaces. The initial L16 and L20 samples were cut to another 4 pieces and irradiated by different energy doses (*D*4 = 140, *D*3 = 175, *D*2 = 233 and *D*1 = 350 J/cm^2).

Fig. 5 shows normalized magnetic moment vs temperature of the L16 (left) and L20 (right) samples before and after laser post-treatment using 4 different energy doses. Different laser energy doses are marked by the value of energy dose applied on Nb surfaces.

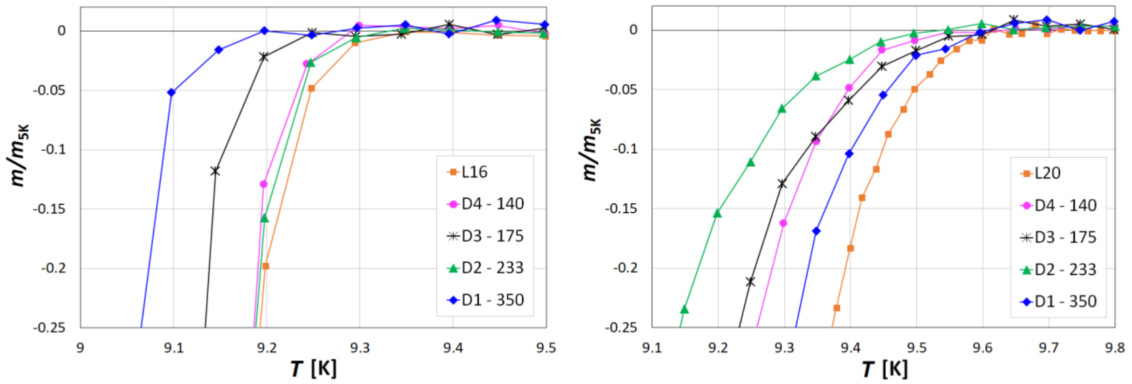

Fig. 5: Normalised magnetic moment vs temperature of the L16 (left) and L20 samples (right) before and after laser post-treatment using 4 different energy doses, The m_{5K} is the magnetic moment at T = 5 K.

Compared to non-irradiated L16 sample, practically no change in T_c was observed after laser irradiation by doses *D*2 and *D*4, but weak reduction in T_c (0.2 K at maximum) was observed after irradiation by *D*1 and *D*3. Compared to non-irradiated L20 sample, the T_c decreased in all 4 cases after laser irradiation (0.3 K at maximum). There was found no correlation between reduction in T_c and the energy dose applied on Nb surfaces or with a change in H_{en} whether considering L16 or L20 sample.

The L20 sample was analysed by EDX to identify the elemental composition of the Nb film. The elemental composition showed that the Nb surface was affected by the oxidation due to the exposure to the ambient air (~10 at.% of Oxygen and ~90 at.% of Nb). As the Nb surfaces are sensitive to be oxidized, the subsequent laser post-treatment could provide diffusion of the oxygen and caused reduction in T_c as observed in [3].

Fig. 6 (a) shows SEM micrograph of the Cu surface of the L16 sample after application of both polishing processes (EP + SUBU5). Pits observed on Cu substrate were replicated on the Nb surface after deposition process (b), with similar diameters, ranging from 0.2 to 3 µm. The Nb surface shows a corrugated morphology related to polycrystalline structure with a size of grains 0.5 - 3 µm.

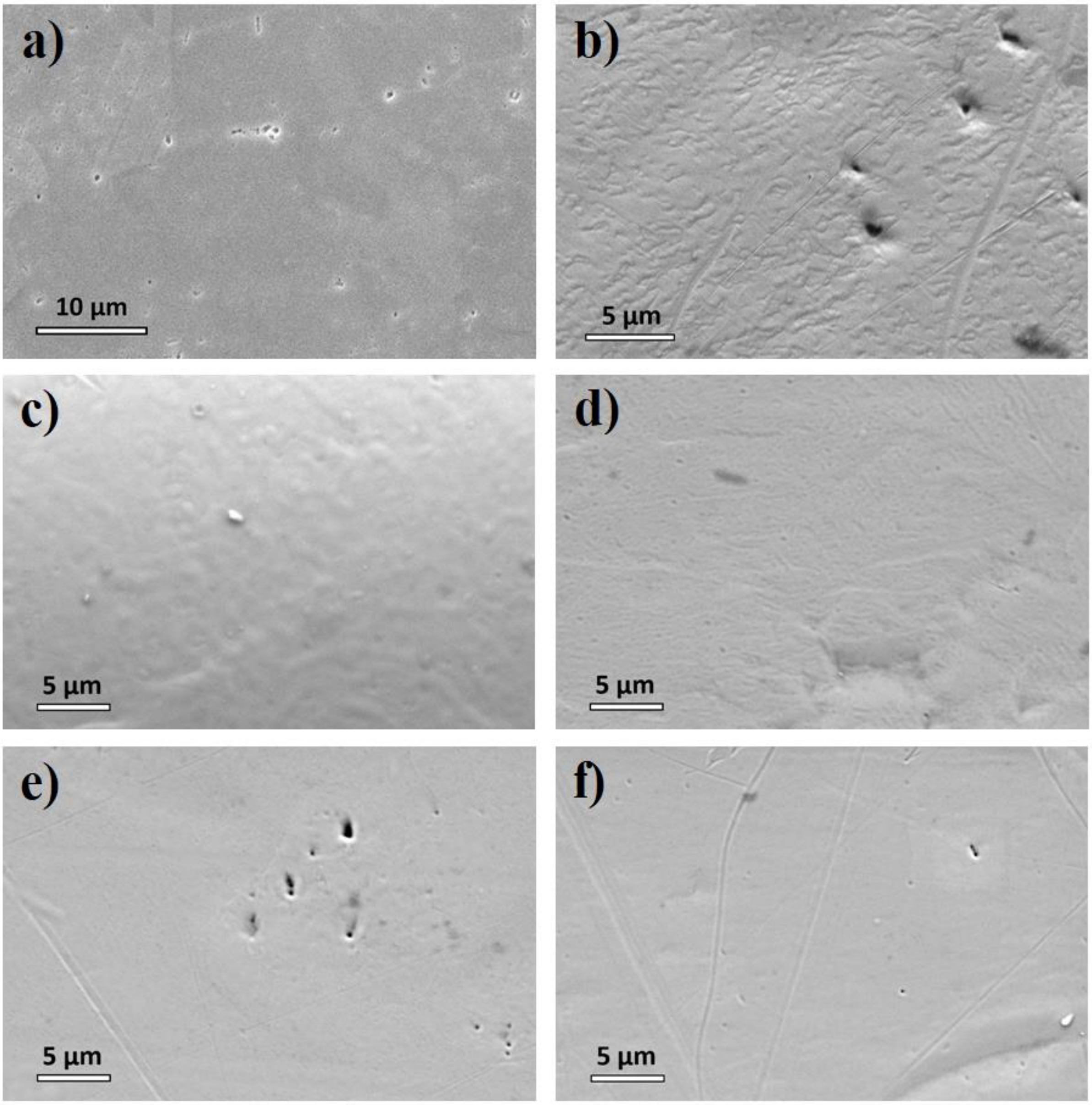

Fig. 6: L16 SEM micrographs of: a) Cu surface after EP+SUBU5 treatment, b) Nb surface before laser irradiation, c) Nb surface after laser irradiation by dose D4 = 140 J/cm^2, d) D3 = 175 J/cm^2, e) D2 = 233 J/cm^2, f) D1 = 350 J/cm^2.

The foot prints of grain boundaries, which are clearly visible on the Nb surface (b), gradually disappeared as the laser dose was increased (c-f), similar as observed in [3]. Picture (c) shows Nb surface after laser irradiation by the lowest laser dose $D4$ = 140 J/cm^2. It is visible that the surface was molten with some level of the initial corrugation still persisting after laser irradiation. To some extent similar corrugation can be observed on the Nb surface irradiated by dose $D3$ = 175 J/cm^2 (d), but with visibly smaller dimensions. No pitting at the $D3$ surface was observed as well. The samples irradiated by doses $D2$ = 233 J/cm^2 (e) and $D1$ = 350 J/cm^2 (f) look well smoothed with practically complete removal of the initial corrugation. However, small holes emerged in both cases, with diameters from 0.1 µm to about 2 µm. Similar features were also observed in [5] [1] after laser irradiation. The explanation of this effect is melting, or even boiling of the Cu under the Nb film, also known as subsurface melting or lid effect [11]. Ejection of rapidly expanding molten Cu can create these holes in the solid Nb film. Melting or boiling of the Cu under the Nb film can occur during the thermal action of the laser because of non-uniform thickness of melted Nb film. Moreover, the boiling point of Cu is only 84 K higher than the melting point of Nb (melting temperature of Cu T_m^{Cu} = 1357.8 K, boiling temperature of Cu T_b^{Cu} = 2835 K, melting temperature of Nb T_m^{Nb} = 2741 K) [12].

By using AFM, the surface roughness R_a of samples was measured before and after laser treatment (Fig. 7). The L16 laser treated samples showed significant reduction of R_a, reduction by approximately one half was observed in all 4 cases. Disappearance of the pitting and reduced surface corrugation resulted in lower R_a after laser irradiation by $D4$ and $D3$. The R_a of the samples irradiated by $D2$ and $D1$ combines positive effect of practically complete removal of the initial corrugation with the negative contribution of holes. This reflects that melting of the Nb surfaces after laser irradiation lead to smoother surfaces, as also observed in the earlier studies [5] [4] [2].

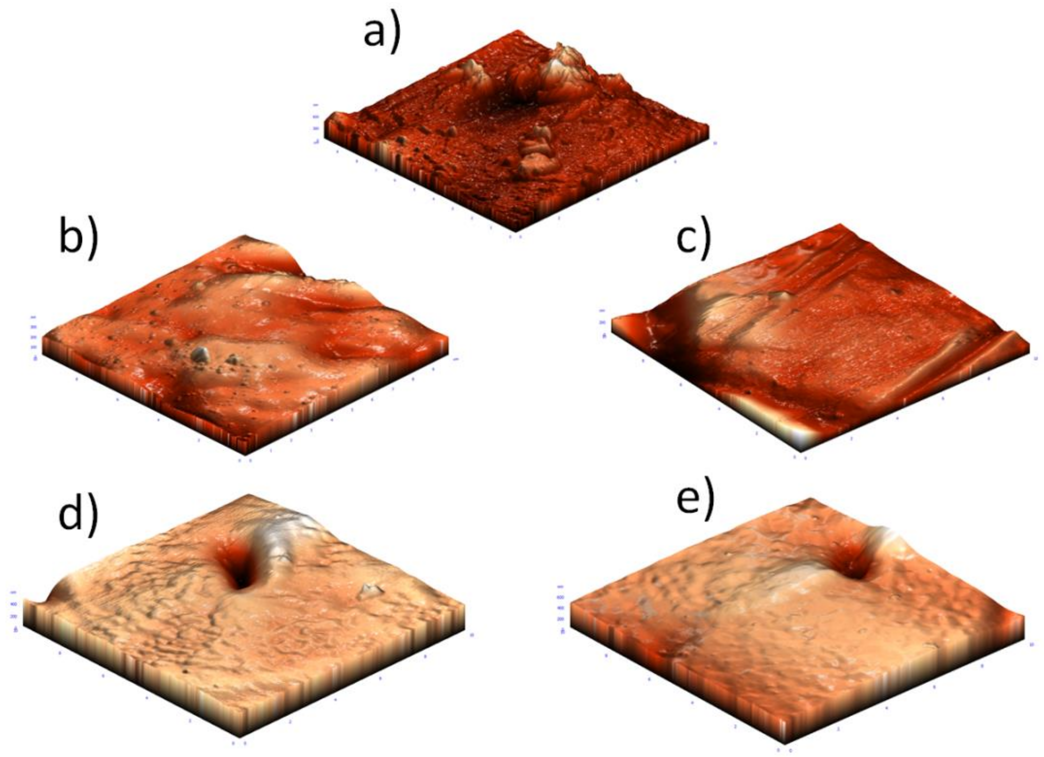

Fig. 7: Surface topography of the L16 surface: a) Non-irradiated b) after laser irradiation by D4 = 140 J/cm², c) D3 = 175 J/cm², d) D2 = 233 J/cm², e) D1 = 350 J/cm².

The XRD analysis was performed to investigate changes in microstructural properties of the Nb samples after laser irradiation. The lattice parameter (a) and Nb crystalline size (L) were obtained from XRD data and using Scherrer equation.

The XRD pattern of the L16 non-irradiated sample showed presence of a dominant diffraction maximum at 70° Nb (211) and weak reflections at other angles. Strong orientation in (211) and characteristic Nb grain size indicate hetero-epitaxial texture of the Nb driven by the underlying Cu structure typical for oxide-free films [13]. After the laser irradiation, the initial orientation of Nb crystallites disappeared and new ones entered with a random orientation in all four cases. After the laser irradiation the size of Nb crystallites decreased from 26 nm to about 20 nm in all four cases. This confirmed that recrystallization was probably only in the first phase - nucleation and subsequent limited growth of the new crystals. The lattice parameter of the non-irradiated sample exhibits a = 0.329755±0.000003 nm close to the lattice parameter of the Nb with zero stress a_0 = 0.3300 nm [14]. The laser irradiation caused practically no change in lattice parameters (~ 0.08% change at maximum) explaining by the relaxation of the residual intrinsic compressive stress [1].

Fig. 8 shows relative comparison between H_{en}, H_p, H_{c2}, surface roughness R_a, lattice parameter a, Nb crystalline size L and M_{rem} in dependence on applied laser dose for L16 samples. The results are normalised to the value of the respective parameter measured for the L16 non-irradiated sample.

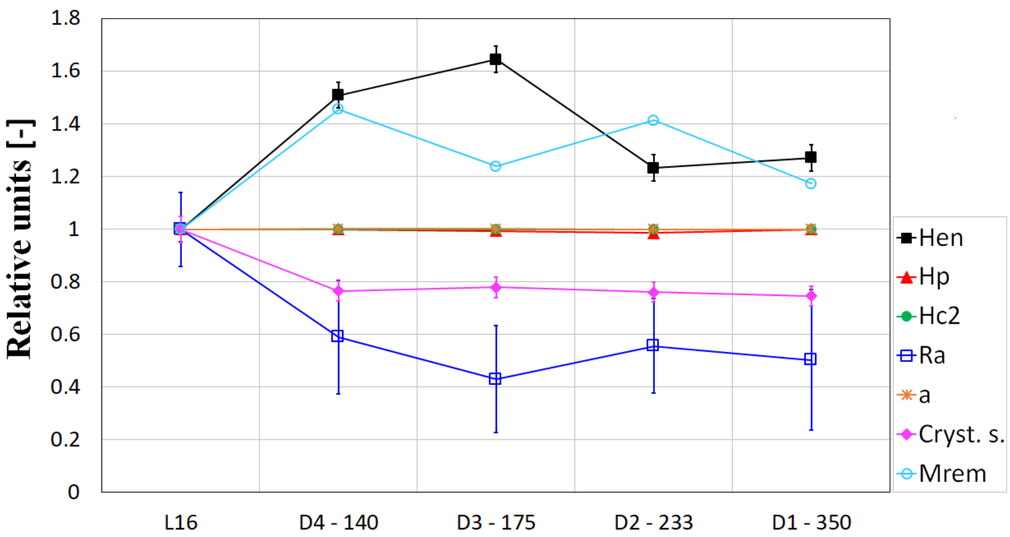

Fig. 8: The relative comparison between H_{en}, H_p, H_{c2}, surface roughness R_a, lattice parameter a, Nb crystalline size L and M_{rem} in dependence of the applied laser dose on Nb surfaces for L16 sample.

As shown from the results, the L16 samples after laser post-treatment showed good correlation between the surface roughness R_a and the first flux entry field H_{en}. As the surface roughness is associated with the surface features observed by the SEM analyses, their impact played the most important role in H_{en} improvement. The L16 sample irradiated by the lowest laser dose $D4$ = 140 J/cm^2 shows relative increase of H_{en} by 51%. This sample is characterized by a smoother surface with some of initial corrugation still persisting after the laser irradiation and by disappearance of the pits. The highest relative increase by 65% was achieved in the sample irradiated by the dose D3, which exhibits smoother surface compared to that of irradiated by laser dose D4 with no occurrence of the pitting. A considerably lower relative increase in H_{en} of 23% and 27% was observed for the samples irradiated by laser doses D2 and D1, respectively. These samples look well smoothed without any of the initial corrugation persisting, but the holes emerged on their surfaces as a result of subsurface melting. The wider magnetisation loops ΔM ($\Delta M = 2M_{rem}$) was measured consistent with the fact that laser irradiation caused finer crystalline structure of the Nb leading to creation of more pinning centres in the film volume.

The samples with the holes on the surfaces, L16 - $D2$ and $D1$ show lower increase of H_{en} compared to those without them. Moreover the sample L20 - $D1$ showed significant decrease of H_{en}, which contains lot of defect including holes. Improvement of the surface morphology after laser irradiation which led to reduced surface roughness has indeed good correlation with a change of H_{en} in the L16 samples. The maximum increase in H_{en} thus seems to be associated with the dose showing the maximum improvement of the surface morphology without further defects formation. In order to calculate the local enhancement of magnetic field caused by surface defect, 2D numerical model was developed.

5. Numerical model of the magnetic field enhancement

As the magnitude of the magnetic field enhancement can be expressed by β factor [15] [16] [17], 2D numerical model was developed employing the Finite Element Method (FEM) in the commercial software Comsol Multiphysics [18]. The enhancement of the local magnetic field was studied on three identified shapes of defects observed on Nb surfaces i.e. delaminated hill-type defect, cracks and pits/holes. Each of these defects causes a magnetic field enhancement and thus represents a place of expected premature vortex penetration into the Nb volume and decrease of H_{en}.

Considering typical dimensions of the defects found on the Nb surfaces, the magnetic field enhancement factor was numerically calculated to $\beta \sim 3.5$ for pits, $\beta \sim 1.7$ for hills and $\beta = 1 - 2$ for cracks depending on their dimensions. The values of β factors calculated by numerical model are valid for most of the defects dimensions found in the sample surfaces. However, as the β factor can still obtain higher or lower values in dependence of defect dimensions, the ratios between the diameters were usually constant leading to constant β factors. Moreover, it was found that defect dimensions are usually connected with a typical peak or edge curvature radii leading to similar enhancement factors whatever taking into account pits, hill or crack.

Conclusion

The research presented in this thesis was aimed to investigate the microstructural and superconducting properties of Nb thin films on Cu substrates, developed for application in SRF cavities. It contributed to the efforts within the research project ARIES-WP15 [19]. The superconducting properties were studied at temperature 4.2 K with the main emphasis on the DC entry field H_{en} as a crucial operational parameter in SRF cavities.

The investigation started with influence of 5 different polishing techniques of Cu substrates and 3 different Nb deposition conditions. In general, the results showed that superconducting properties of the samples were dominantly given by the Nb deposition conditions (the best results of STFC samples) with a weak effect of Cu substrate polishing.

The series of 5 samples (INFN) were further irradiated by Nd:YAG laser using constant energy dose D = 70 J/cm^2. The laser post-treatment caused smoother surfaces with visibly melted Nb film and increase of H_{en} in all five samples. The largest increase of H_{en} was observed at the samples showing the most improved surface morphology, an increase by up to 19% was observed.

The Nb surfaces of the two samples (L16 and L20) were irradiated by laser using 4 different energy doses (D4 = 140, D3 = 175, D2 = 233 and D1 = 350 J/cm^2). As a result, the L16 sample showed good correlation between the surface roughness R_a and the first flux entry field H_{en} after laser post-treatment. The highest relative increase by 65% (using D3) was achieved in the sample showing well smoothed surface and no occurrence of pitting. The laser irradiation caused also reduction of Nb crystallites size from 26 nm to about 20 nm in all four cases. The wider magnetisation loops ΔM are consistent with the fact that laser irradiation caused finer crystalline structure of the Nb leading to creation of more pinning centres in the film volume. In the case of L20 sample, the highest relative increase of H_{en} was 45% (using D2) in the sample showing well smoothed surface, no signs of persisted pits but cracks emerged after laser irradiation. Sample irradiated by the highest laser dose D1 exhibits significantly reduced H_{en} (-83%) showing smooth surface with a lot of cracks, holes and highest degree of Nb delamination. The values of H_p, H_{c2} and lattice parameter were not visibly changed after laser irradiation in both L16 and L20 samples.

As the DC superconducting measurements are very surface-sensitive, the increase in H_{en} after laser irradiation was not surprising due to observed smoother surfaces and reduced surface defects. The results show that the first flux entry field H_{en} was mostly influenced by the locally enhanced magnetic field created by several sources such as grain boundaries [16], pits [17], micro-particles [20], microscopic surface roughness [21] or crystalline defects [22]. As the laser irradiation led to increase compactness/uniformity of the grains at the surfaces, the enhancement of the local magnetic field at the grain boundaries decreased. However, the presence of the pits or holes has much bigger effect on enhancement of the magnetic field, as supported by the numerical model and analytical study [17]. The maximum magnetic field enhancement factor was numerically calculated to β ~ 3.5 for pits, β ~ 1.7 for hills and β = 1 - 2 for cracks depending on their dimensions. These values of β factors are valid for most of the defect dimensions found in the sample surfaces. The samples which showed the holes on the surfaces (L16 - D2 and D1) showed indeed smaller increase of H_{en} compared to L16-D3 and D4. The holes emerged on the surface of the L20-D1 sample showed significant decrease of H_{en}.

In summary, the highlights and new findings provided by this thesis are:

a) The microstructural and DC superconducting properties of the Nb/Cu samples were studied according to 5 techniques of Cu substrate polishing and 3 different Nb deposition conditions.

b) Deposition parameters showed major effect on superconducting properties rather than different Cu substrate polishing methods. The samples deposited in deposition conditions used at STFC showed in average the best results of H_{en}.

c) Compared to previous studies, 10 times higher laser energy doses were applied on Nb surfaces with the investigation of superconducting and microstructural properties.

d) The effects of laser post-treatment on superconducting and microstructural properties were studied using 14 differently prepared Nb/Cu samples and laser energy doses ranging from 70 to 350 J/cm^2.

e) By using laser post-treatment, majority of the surface defects was removed and the first magnetic flux entry field H_{en} increased by up to 65% (using energy dose 175 J/cm^2).

f) The highest energy dose applied on Nb surfaces (350 J/cm^2) caused formation of new defects such as cracks, holes and Nb film delamination and resulted in lower increase of H_{en} or even its reduction.

g) In most cases, the laser post-treatment of the Nb/Cu samples causes slight reduction of critical temperature T_c, reduction in surface roughness R_a, reduction in Nb crystallite size L and increase in magnetization loop width ΔM.

h) It was found that the hole-type defects, pits after SUBU5 applied on Cu and holes after laser irradiation, cause the highest enhancement of local magnetic field that leads to reduction of the first magnetic flux entry field H_{en}.

References

[1] E. Radicioni, C. Benvenuti, M. Bianconi and L. Correra, “Laser annealing of Nb coatings for superconducting RF accelerating cavities,” *Nuclear Inst. and Methods in Physics Research,* no. 365(1), pp. 28-35, 1995.

[2] L. Zhao, J. M. Klopf, C. E. Reece and M. J. Kelley, “Laser polishing for topography management of accelerator cavity surfaces,” *Materialwissenschaft und Werkstofftechnik,* no. 46(7), pp. 675-685, 2015.

[3] Y. Yang, X. Lu, W. Tan, L. Xiao, L. Zhu and D. Xie, “Study on laser annealing on niobium films deposited on copper for RF superconducting cavities,” *Nuclear Inst. and Methods in Physics Research,* no. A 964, 2020.

[4] A. Cubero, E. Martinez, L. A. Angurel, G. F. de-la-Fuente, N. R, H. Legall, J. Kruger and J. Bonse, “Effects of laser-induced periodic surface structures on the superconducting properties of Niobium,” *Appl. Surf. Sci.,* no. 508, 2020.

[5] A. Medvids, P. Onufrijevs, J. Kaupuzs, I. Grasea, O. B. Malyshev, R. Valizadeh, A.

Žunda and J. Padgurskas, “Improvement of Nb/Cu adhesion and increase of Nb crystal size by laser radiation,” *Appl. Surf. Sci.,* no. 525, 2020.

[6] O. Kugeler, C. Z. Antoine, E. Seiler, F.Gömöry, A. Medvids, P. Onufrijevs, C. Pira, E. Chyhyrynets, O. B. Malyshev, R. Valizadeh, R. Ries, A. Sublet, M. Vogel, S. Leith, X. Jiang and D. Turner, “ARIES Deliverable Report D15.1 - Final report WP15,” no. M21, 2021.

[7] A. S. Dhavale, P. Dhakal, A. A. Polanskii and G. Ciovati, “Flux pinning characteristics in cylindrical niobium samples used for superconducting radio frequency cavity fabrication,” *Supercond. Sci. Technol.,* vol. 25, no. 065014, 2012.

[8] S. B. Roy, G. R. Myneni and V. C. Sahni, “On the reliable determination of the magnetic field for first flux-line penetration in technical niobium material,” *Supercond. Sci.technol.,* vol. 21, no. 065002, 2008.

[9] R. Ries, E. Seiler, F. Gömöry, A. Medvids, C. Pira and O. B. Malyshev, “Superconducting properties and surface roughness of thin Nb samples fabricated for SRF applications,” *Journal of Physics Conference Series,* no. 1559:012040, 2020.

[10] C. Pira et al, “ARIES Deliverable Report D15.1 - Evaluation of Cleaning Process,” no. M12, 2018.

[11] A. Medvids and P. M. Lytvyn, “Dynamic of Laser Ablation in SiC,” *Materials Science Forum,* no. 411, pp. 457-460, 2004.

[12] R. Ries, E. Seiler, F. Gömöry, A. Medvids, P. Onufrijevs, C. Pira, E. Chyhyrynets, O. B. Malyshev and R. Valizadeh, “Improvement of the first flux entry field by laser post-treatment of the thin Nb film on Cu,” *Supercond. Sci. Technol.,* 2021.

[13] A.-M. Valente-Feliciano, “Superconducting RF material other than bulk niobium: a review,” *Supercond. Sci. Technol.,* vol. 29, no. 113002, 2016.

[14] R. A. Amos, P. E. Breyer, H. H. Huang and A. W. Lichtenberger, “Stress and source conditions of DC magnetron sputtered Nb films,” *IEEE Trans. Appl. Supercond.,* no. 5(2), pp. 2326-2329, 1995.

[15] C. Z. Antoine, “Materials and surface aspects in the development of SRF Niobium cavities,” *European Coordination for Accelerator Research and Development EuCARD,* no. BOO-001, 2012.

[16] J. Knobloch, R. L. Geng, M. Liepe and H. Padamsee, “High-field Q slope in superconducting cavities due to magnetic field enhancement at grain boundaries,” *Proceedings of the 1999 Workshop on RF Superconductivity, New Mexico, USA,* 1999.

[17] V. Shemelin and H. Padamsee, “Magnetic field enhancement at pits and bumps on the surface of superconducting cavities,” *Proc. TTC-Report 7,* 2008.

[18] COMSOL Multiphysics® v. 5.4., “www.comsol.com,” COMSOL AB, Stockholm, Sweden. [Online].

[19] Accelerator Research and Innovation for European Science and Society, “https://aries.web.cern.ch/home,” CERN. [Online].

[20] H. Padamsee, “50 years of success for SRF accelerators – a review,” *Supercond. Sci. Technol.,* vol. 053003, no. 30, 2017.

[21] G. Wu, M. Ge, P. Kneisel, K. Zhao, L. Cooley, J. Ozelis, D. Sergatskov and C. Cooper, “Investigations of Surface Quality and SRF Cavity Performance,” *Applied Superconductiity Conference USA,* 2012.

[22] C. Z. Antoine, “Influence of crystalline structure on rf dissipation in superconducting niobium,” *Phys. Rev. Accel. Beams,* vol. 034801, no. 22, 2019.

List of publications

Publications in CC database:

1. Seiler, E., Gömöry, F., **Ries, R**., and Vojenčiak, M.: Analysis of critical current anisotropy in commercial coated conductors in terms of the maximum entropy approach, Supercond. Sci Technol. 32 (2019) 095004. (IF 2.489)
2. Leith, S., Vogel, M., Seiler, E., **Ries, R**., and Jiang, X.: Superconducting NbN thin films for use in superconducting radio frequency cavities, Supercond. Sci Technol. 34 (2021) 025006. (IF 3.067)
3. **Ries, R**., Seiler, E., Gömöry, F., Medvids, A., Onufrijevs, P., Pira, C., Chyhyrynets, E., Malyshev, O.B., and Valizadeh, R.: Improvement of the first flux entry field by laser post-treatment of the thin Nb film on Cu, Supercond. Sci Technol. 34 (2021) 065001. (IF 3.067)

Publications in SCOPUS database:

1. **Ries, R**., Seiler, E., Gömöry, F., Medvids, A., Pira, C., and Malyshev, O.B.: Superconducting properties and surface roughness of thin Nb samples fabricated for SRF applications, J. Phys.: Conf. Ser. 1559 (2020) 012040.

Conference participations:

1. Gömöry, F., Solovyov, M., Šouc, J., Vojenčiak, M., Seiler, E., Frolek, L., and **Ries, R**.: Electromagnetic and thermal modeling of small coil made from HTS round cable. In: CHATS on Applied Supercond. 2017. Sendai 2017.
2. Mikulášová, E., Gömöry, F., **Ries, R**., Kujovič, T., Mošať, M., and Sojková, M.: Low temperature bonding of superconducting tapes covered by Ag layer. In: Workshop on Coated Conductors for Applications 2018. Vienna 2018. Poster.
3. **Ries, R**., Mošať, M., Gömöry, F., Vojenčiak, M., Seiler, E., Pekarčíková, M., Cuninková, E., and Mišík, J.: Characterizing of superconducting tape quality by measuring magnetic AC susceptibility. In: Workshop on Coated Conductors for Applications 2018. Vienna 2018. Poster.
4. Seiler, E., **Ries, R**., Gömöry, F., and Vojenčiak, M.: Angular Ic anisotropy and pinning properties of coated conductors in moderate magnetic fields at temperatures close to 77 K. In: Workshop on Coated Conductors for Applications 2018. Vienna 2018. Poster.
5. Seiler, E., Gömöry, F., **Ries, R**., and Vojenčiak, M.: Critical current anisotropy of industrial coated conductors close to 77 K. In: EUCAS 2019. Glasgow 2019. Poster
6. **Ries, R**., Seiler, E., Medvids, A., Malyshev, O.B., Valizadeh, R., Pira, C., Vogel, M., Leith, S., Jiang, X., Sublet, A., Antoine, C.Z., and Kugeler, O.: Correlation between first flux entry field and surface roughness of Nb samples. In EUCAS 2019. Poster.

7. Leith, S., Vogel, M., Jiang, X., Seiler, E., **Ries, R**., Pira, C., Antoine, C.Z., Katasevs, A., Kaupuzs, J., Medvids, A., Onufrijevs, P., Kugeler, O., Malyshev, O.B., Valizadeh, R., and Sublet, A.: Deposition parameter effects on niobium nitride (NbN) thin films deposited onto copper substrates with DC magnetron sputtering. In 19th Int. Conf. on RF Superconductivity SRF 2019. ISBN: 978-3-95450-211-0 Dresden: JACoW Publ. 2019, pp. 947-951.
8. Pira, C., Antoine, C.Z., Jiang, X., Leith, S., Vogel, M., Katasevs, A., Kaupuzs, J., Medvids, A., Onufrijevs, P., Kugeler, O., Malyshev, O.B., Valizadeh, **R., Ries**, R., Seiler, E., Sublet, A.: Impact of the Cu substrate surface preparation on the morphological, superconductive and RF properties of the Nb superconductive coatings. In 19th Int. Conf. on RF Superconductivity SRF 2019. ISBN: 978-3-95450-211-0 Dresden: JACoW Publ. 2019, pp. 937 – 942.
9. Pardo, E., Kováč, J., Kopera, L., **Ries, R**., Grilli, F., Berberich, E., and Reis, T.: AC loss in the REBCO stator of a 1 MW motor for aviation. In: 33th Inter. Symp. on Supercond. - ISS 2020. Tsukuba 2020.

Citations:

Seiler, E., Gömöry, F., **Ries, R**., M., and Vojenčiak, M.: Analysis of critical current anisotropy in commercial coated conductors in terms of the maximum entropy approach, Supercond. Sci Technol. 32 (2019) 095004.

1. Kapolka, M.: Supercond. Sci Technol. 33 (2020) 044019.